

NACA TN 3521

# NATIONAL ADVISORY COMMITTEE FOR AERONAUTICS

TECHNICAL NOTE 3521

A COMPARISON OF THE MEASURED AND PREDICTED LATERAL  
OSCILLATORY CHARACTERISTICS OF A 35°  
SWEPT-WING FIGHTER AIRPLANE

By Walter E. McNeill and George E. Cooper

Ames Aeronautical Laboratory  
Moffett Field, Calif.



Washington

August 1955

F

NATIONAL ADVISORY COMMITTEE FOR AERONAUTICS

---

TECHNICAL NOTE 3521

---

A COMPARISON OF THE MEASURED AND PREDICTED LATERAL  
OSCILLATORY CHARACTERISTICS OF A  $35^\circ$   
SWEPT-WING FIGHTER AIRPLANE<sup>1</sup>

By Walter E. McNeill and George E. Cooper

SUMMARY

Results of tests of a  $35^\circ$  swept-wing fighter airplane, during which lateral oscillations were performed over a Mach number range from 0.41 to 0.79 at a pressure altitude of 10,000 feet and from 0.49 to 1.04 at 35,000 feet, are presented in this report. Experimental and computed values for the period of the lateral oscillation and time required to damp to half amplitude are shown. One sample oscillation time history is included for each test altitude.

The airplane was found to be laterally stable, statically and dynamically, throughout the range of speeds tested. At both altitudes, the variation with Mach number of the period of the lateral oscillation was satisfactorily predicted from available and estimated aerodynamic and mass parameters. The time required to damp to half amplitude, as measured from flight at both altitudes, varied with Mach number in essentially the same manner as predicted from computations. The measured damping was somewhat better than that obtained from computations for the altitude of 35,000 feet, particularly at a Mach number of 0.92. An increase in time to damp to half amplitude was noted between Mach numbers of 0.95 and 1.04.

INTRODUCTION

As part of a general research program concerned with the lateral dynamic stability and handling characteristics of high-speed, high-altitude airplanes, the Ames Aeronautical Laboratory of the NACA has tested a  $35^\circ$  swept-wing fighter airplane through a wide range of flight speeds and altitudes.

The purpose of this report is to present results of tests of the lateral oscillatory characteristics made during a series of four flights. Comparisons are included of the computed variation of period and damping of the lateral oscillation with the measured values. These comparisons

---

<sup>1</sup>Supersedes recently declassified NACA RM A51C28 by Walter E. McNeill and George E. Cooper.

---

indicate the accuracy with which the oscillatory behavior of an airplane can be predicted under various flight conditions using available or estimated mass parameters and stability derivatives, and neglecting such effects as aeroelasticity and unsteady lift.

## SYMBOLS

$C_L$	lift coefficient, $\frac{\text{lift}}{qS}$
$C_{L_\alpha}$	$\frac{\partial C_L}{\partial \alpha}$ , per deg
$C_Y$	lateral-force coefficient, $\frac{\text{lateral force}}{qS}$
$C_{Y_\beta}$	$\frac{\partial C_Y}{\partial \beta}$ , per radian
$C_{Y_p}$	$\frac{\partial C_Y}{\partial \frac{pb}{2V}}$ , per radian
$C_{Y_r}$	$\frac{\partial C_Y}{\partial \frac{rb}{2V}}$ , per radian
$C_l$	rolling-moment coefficient, $\frac{\text{rolling moment}}{qSb}$
$C_{l_\beta}$	$\frac{\partial C_l}{\partial \beta}$ , per radian
$C_{l_p}$	$\frac{\partial C_l}{\partial \frac{pb}{2V}}$ , per radian
$C_{l_r}$	$\frac{\partial C_l}{\partial \frac{rb}{2V}}$ , per radian
$C_n$	yawing-moment coefficient, $\frac{\text{yawing moment}}{qSb}$
$C_{n_\beta}$	$\frac{\partial C_n}{\partial \beta}$ , per radian
$C_{n_p}$	$\frac{\partial C_n}{\partial \frac{pb}{2V}}$ , per radian

$C_{nr}$	$\frac{\partial C_n}{r b} \frac{\partial}{\partial 2V}$ , per radian
$I_x$	moment of inertia about flight-path axis, slug-ft <sup>2</sup>
$I_z$	moment of inertia about axis normal to flight path in the plane of symmetry, slug-ft <sup>2</sup>
$M$	Mach number
$P$	period of oscillation, sec
$S$	wing area, sq ft
$T_{1/2}$	time to damp to half amplitude, sec
$V$	true airspeed, ft/sec
$W$	weight of airplane, lb
$b$	wing span, ft
$h_p$	pressure altitude, ft
$l_{vr}$	distance parallel to longitudinal reference axis from center of gravity of the airplane to center of pressure of vertical tail in yaw, ft
$p$	rolling angular velocity, radians/sec
$q$	dynamic pressure, lb/sq ft
$r$	yawing angular velocity, radians/sec
$z_{vr}$	normal distance from longitudinal reference axis to center of pressure of vertical tail in yaw, ft
$\alpha$	angle of attack of longitudinal reference axis, deg
$\alpha_0$	angle of attack of longitudinal reference axis for zero lift, deg
$\beta$	angle of sideslip, radians
$\Gamma$	dihedral angle, radians
$\epsilon$	angle between longitudinal reference axis and principal axis of airplane, positive when reference axis is above principal axis at nose, deg

$\sigma$	sidewash angle at vertical tail resulting from the wing in rolling flow, positive for positive lateral force, radians
$\phi$	angle of bank, radians
$\frac{ \phi }{ \beta }$	ratio of amplitude of angle of bank to amplitude of sideslip angle for the oscillatory mode

#### Subscripts

h	contributed by horizontal tail
i+f	contributed by fuselage and wing-fuselage interference
M	pertaining to a given Mach number
v	contributed by vertical tail
w	contributed by wing
W.T.	obtained from wind-tunnel tests

#### INSTRUMENTATION AND FLIGHT TECHNIQUE

The general arrangement of the test airplane is shown by a photograph (fig. 1) and a two-view drawing (fig. 2). The principal dimensions are listed in table I.

Standard NACA recording instruments were used to measure angle of sideslip, rolling and yawing velocities, pressure altitude, and airspeed. Aileron and rudder deflections were recorded by NACA instruments as well as on separate channels of a 36-channel oscillograph. The rudder deflection was known to an accuracy of  $0.1^\circ$ , while the aileron deflection was known within  $0.3^\circ$ . The nose-boom airspeed system described in reference 1 was used to determine Mach number and the static and dynamic pressure. The records were synchronized by a 1/10-second instrument timer.

At a pressure altitude of 10,000 feet, lateral oscillation maneuvers were performed through a range of Mach numbers from 0.41 to 0.79. At an altitude of 35,000 feet, oscillations were performed at Mach numbers from 0.49 to 1.04.

All oscillations performed at 10,000 feet were excited by returns from steady sideslips. At 35,000 feet, the airplane was disturbed both by returns from steady sideslips and by abruptly deflecting the rudder and returning it to neutral, except at Mach numbers above 1.02, where

rudder kicks alone were used. During all test runs below a Mach number of 1.0, the rudder and ailerons were held essentially fixed following their return to trim positions with the aid of chains which prevented the pilot's moving his controls beyond a predetermined point. At Mach numbers above 1.0, chains were used on the rudder pedals only.

All oscillations were performed in the clean condition and in level flight, with the exception of those at Mach numbers above 0.92 where dive angles up to  $36^\circ$  were required.

## RESULTS AND DISCUSSION

Typical time histories of indicated airspeed, pressure altitude, side-slip angle, rolling velocity, yawing velocity, total aileron deflection, and rudder deflection are shown in figure 3 for a Mach number of 0.79 at a pressure altitude of 10,000 feet. Figure 4 presents time histories of the same quantities for an average Mach number of 1.04 at about 35,000 feet.

The results of data obtained during similar lateral oscillations at altitudes of 10,000 and 35,000 feet are summarized in figure 5 in the form of period and time required to damp to half amplitude expressed as functions of Mach number.

For comparison with the experimental results, curves of computed values for period and damping also are shown in figure 5. These values are solutions to stability quartics derived from the lateral equations of motion presented in reference 2. The mass distribution and dimensional data used in computing period and damping were furnished by the manufacturer. The methods used to measure or estimate the variation of the stability derivatives with Mach number and lift coefficient are summarized in the appendix. All lateral derivatives were corrected for compressibility effects according to the Prandtl-Glauert rule, as outlined in the appendix, from  $M = 0$  to  $M = 0.9$ . Each derivative was then plotted as a function of Mach number and the resulting curve was extrapolated at a constant slope from  $M = 0.9$  to  $M = 1.0$ . Table II presents the values of the parameters used in computing period and damping at each Mach number considered at altitudes of 10,000 and 35,000 feet, together with the resulting values of  $P$ ,  $T_{1/2}$ , and  $\frac{|\phi|}{|\beta|}$ . The lift coefficients shown in table II are representative of the flight values except for Mach numbers greater than 0.95, where a deviation of less than 15 percent would be expected. Because of the small range of angle of attack involved (less than  $5^\circ$ ), the rolling and yawing moments of inertia were assumed constant at the values given beneath table II.

Figure 5 indicates that reasonably close correspondence (within 8 percent) was obtained between the variation with Mach number of computed and measured values of period at pressure altitudes of 10,000 and 35,000

feet. The measured period is observed to decrease less rapidly with increasing Mach number than did the computed value at 35,000 feet. At 10,000 feet the opposite trend is seen; that is, the experimental value of the period decreased slightly more rapidly than did the computed value as Mach number was increased. No explanation for this phenomenon is apparent.

Close agreement (within 7 percent) existed between the measured and computed values for  $T_{1/2}$  at Mach numbers below 0.6 at 10,000 feet. Above  $M = 0.6$  the flight-test values for  $T_{1/2}$  became increasingly higher than the computed values as the Mach number was increased. At 35,000 feet the measured values for  $T_{1/2}$  were somewhat lower than the computed values throughout the major portion of the Mach number range tested (0.49 to 1.04), with the best agreement occurring at low speed. Above  $M = 0.8$  the experimental value of  $T_{1/2}$  decreased more rapidly, reaching a maximum deviation of about 20 percent from the computed curve at  $M = 0.92$ , then changed its slope gradually from negative to positive up to  $M = 1.04$ . Due to the scatter of test points at Mach numbers above 1.0, it is difficult to determine more than the general trend indicated in figure 5.

It is evident that a good prediction was made of the lateral period and damping of the test airplane for the range of lift coefficients considered in the computations (0.076 to 0.412) using  $C_{n_p}$  and  $C_{l_p}$  for the wing alone, as shown by the dashed curves in figure 5. In this instance, nothing was gained by considering the contributions of the vertical tail in addition to the wing, as shown by the low and high Mach number points for which  $C_{n_p}$  and  $C_{l_p}$  were computed by the methods of reference 3. As the lift coefficient of the airplane is increased, however, the vertical-tail contribution to  $C_{n_p}$  becomes quite large and could be included as shown in the appendix.

Figure 6 presents the above flight information as the relationship between period and time to damp to half amplitude for each altitude, together with the corresponding computed values. Good agreement between the measured and computed period-damping relationships is again demonstrated by this method of presentation, particularly for the altitude of 10,000 feet below a Mach number of 0.6. As in figure 5, figure 6 shows a lower experimental value of  $T_{1/2}$  for 35,000 feet at all Mach numbers, particularly at  $M = 0.9$ , in relation to the computed values.

The Armed Services lateral-oscillation specification which applied at the time of these tests (ref. 4) is shown in figure 6 for comparison with the characteristics of the test airplane. It is shown that the lateral oscillatory characteristics of the test airplane at 35,000 feet were entirely within the unsatisfactory region defined in reference 4. The same figure shows that the airplane, at 10,000 feet, exhibited borderline characteristics with respect to the requirements of reference 4 except at Mach numbers between 0.54 and 0.79 where the period-damping relationships were in the satisfactory region. The computations indicate that for low Mach numbers, near 0.35, characteristics exist which are satisfactory under the requirements of reference 4.

According to the pilot's comments, the lateral oscillatory characteristics of the test airplane were generally satisfactory at 10,000 feet. At 35,000 feet, the oscillations were somewhat objectionable, partly because of the increased rolling that was present (see table III) and partly because of the noticeably decreased damping which was especially apparent in rough air. Rough air tended to prolong the oscillations at 10,000 feet as well but, since there was considerably less rolling present at comparable Mach numbers, the motions were not considered so objectionable as those experienced at the higher altitude.

Results of other lateral flying qualities investigations conducted at the Ames Aeronautical Laboratory (see ref. 5) have indicated the possibility of the use of the ratio of amplitude of angle of bank to amplitude of sideslip angle for the oscillatory mode  $\frac{|\phi|}{|\beta|}$  as a criterion for satisfactory lateral oscillatory characteristics of fighter-type airplanes.

Measured values of  $\frac{|\phi|}{|\beta|}$  are presented, in addition to period and time to damp to half amplitude, in table III for the Mach number ranges covered at the test altitudes of 10,000 and 35,000 feet.

Computed values of  $\frac{|\phi|}{|\beta|}$  are shown in table II for Mach numbers considered at 10,000 and 35,000 feet. Through the speed ranges covered at both altitudes,  $\frac{|\phi|}{|\beta|}$  for the test airplane was predicted with less accuracy than were period and damping.

### CONCLUSIONS

1. In general, the lateral oscillatory characteristics of the test airplane were closely predicted from information based on wind-tunnel tests, although unsteady lift and aeroelastic effects were neglected.
2. Throughout the range of Mach numbers tested (0.41 to 1.04) the airplane was laterally stable both statically and dynamically.
3. The period of the lateral oscillation varied smoothly with Mach number over the range tested and was adequately represented by computed values at both test altitudes, with no error greater than 8 percent.
4. The time required for the lateral oscillation to damp to half amplitude at test altitudes of 10,000 and 35,000 feet decreased with Mach number in essentially the same manner as indicated by computations, except at 35,000 feet where the measured value of  $T_{1/2}$  began to increase with Mach number above  $M = 0.95$ .



## APPENDIX

## ESTIMATION OF LATERAL-STABILITY DERIVATIVES

## FOR THE TEST AIRPLANE

The values presented in table II for the lift-curve slope, angle of attack at zero lift, and the static lateral-stability derivatives were obtained from wind-tunnel or other force-test methods and corrected for compressibility effects where tests did not cover the Mach number range considered in this report. The rotary derivatives were estimated by published theoretical methods applicable to swept wings.

The procedures used in determination of the aerodynamic parameters and stability derivatives considered in this report are presented below.

## Longitudinal Trim Parameters

Variation of lift-curve slope,  $C_{L\alpha}$ , with Mach number was determined from the results of subsonic tests in the Ames 16-foot wind tunnel and the Southern California Cooperative Wind Tunnel to a Mach number of 0.94 and supplemented by transonic bump tests to a Mach number of 1.06.

Angle of attack for zero lift,  $\alpha_0$ , was taken from unpublished results of NACA wing-flow tests.

## Static Lateral-Stability Derivatives

Lateral force due to sideslip.- The coefficient of lateral force due to sideslip,  $C_{Y\beta}$ , was obtained from wind-tunnel data taken at  $M = 0.16$  for a 0.20-scale model of the test airplane, both complete and with tail removed. Changes in  $C_{Y\beta}$  due to increasing Mach number were computed by applying equation (1) of <sup>6</sup>reference 6 to the contribution of the vertical tail assuming that the tail-off value did not vary with Mach number.

Yawing moment due to sideslip.- The coefficient of yawing moment due to sideslip,  $C_{n\beta}$ , was obtained from wind-tunnel data taken at  $M = 0.16$  and corrected for higher Mach numbers in a manner identical with that used for  $C_{Y\beta}$ .

Rolling moment due to sideslip.- The coefficient of rolling moment due to sideslip,  $C_{l\beta}$ , was determined from wind-tunnel data obtained at  $M = 0.16$  at angles of attack of  $0^\circ$  and  $8^\circ$  for the complete 0.20-scale model, the model with tail removed, and the wing alone.

The wing contribution to  $C_{l\beta}$  was broken down into two parts as follows:

$$(C_{l\beta})_w = \left[ \frac{\left( \frac{\partial C_{l\beta_w}}{\partial C_L} \right)_M}{\left( \frac{\partial C_{l\beta_w}}{\partial C_L} \right)_{M=0}} \right]_{\text{reference 6}} \left[ \left( \frac{\partial C_{l\beta_w}}{\partial C_L} \right)_{C_L} \right]_{M=0.16}^{W.T.} +$$

$$\left[ \frac{\left( \frac{\partial C_{l\beta_w}}{\partial \Gamma} \right)_M}{\left( \frac{\partial C_{l\beta_w}}{\partial \Gamma} \right)_{M=0}} \right]_{\text{reference 7}} \left[ \left( \frac{\partial C_{l\beta_w}}{\partial \Gamma} \right)_\Gamma \right]_{M=0.16}^{W.T.} \quad (A1)$$

At  $C_L = 0$ , the dihedral effect of the wing was assumed to be due entirely to the geometric dihedral angle, reducing the first term of equation (A1) to zero. The second term of equation (A1) was then assumed constant with  $C_L$  at a given Mach number, enabling the first term to be evaluated at lift coefficients greater than zero. The compressibility corrections indicated in equation (A1) were applied assuming that test results obtained at  $M = 0.16$  were essentially those at  $M = 0$ .

The contribution of the vertical tail to  $C_{l\beta}$  was determined from the tail-on and tail-off data at angles of attack of  $0^\circ$  and  $8^\circ$  and corrected for higher Mach numbers using the method applied to the tail contribution to  $C_{Y\beta}$ .

The increment of  $C_{l\beta}$  due to interference and the fuselage was obtained from wind-tunnel tests of the wing alone and the wing-fuselage combination at both  $0^\circ$  and  $8^\circ$  angles of attack and was assumed constant with Mach number.

For the entire airplane,  $C_{l\beta}$  was determined in the following manner:

$$C_{l\beta} = (C_{l\beta})_w + (C_{l\beta})_v + (C_{l\beta})_{i+f} \quad (A2)$$

#### Rotary Derivatives

Rolling moment due to rolling.- The rolling-moment coefficient due to rolling velocity,  $C_{lp}$ , was determined as a function of Mach number for the wing alone by application of figure 5 of reference 7.

The contribution of the horizontal tail was determined by the method applied to the wing. To express the values of  $C_{l_p}$  for the horizontal tail in terms of wing area, span, and wing-tip helix angle, the values obtained from figure 5 of reference 7 were corrected by the following method:

$$(C_{l_p})_h = \frac{S_h b h^2}{S_b^2} \left[ (C_{l_p})_h \right]_{\text{reference 7}} \quad (A3)$$

The contribution of the vertical tail was determined by the method presented in reference 3, using a value of sidewash parameter  $\left( \frac{\partial \sigma}{\partial \frac{pb}{2V}} \right)$  equal to 0.248, obtained from unpublished results of a theoretical investigation and tests conducted in the Langley stability tunnel.

The contributions of the wing, horizontal tail, and vertical tail were added algebraically to obtain the estimated values of  $C_{l_p}$  for the test airplane at different Mach numbers and lift coefficients:

$$C_{l_p} = (C_{l_p})_w + (C_{l_p})_h + (C_{l_p})_v \quad (A4)$$

Yawing moment due to rolling.- The yawing-moment coefficient due to rolling velocity,  $C_{n_p}$ , was determined as a function of lift coefficient according to equation (31) and figure 25 of reference 8 for the wing alone. The variation thus obtained was corrected for compressibility effects by application of equation (3) of reference 6.

The contribution of the vertical tail was determined by the method presented in reference 3 and added algebraically to the wing contribution to obtain  $C_{n_p}$  for the entire airplane:

$$C_{n_p} = (C_{n_p})_w + (C_{n_p})_v \quad (A5)$$

In the discussion it was noted that use of  $C_{l_p}$  and  $C_{n_p}$  for the wing alone in the computations gave adequate agreement with experimental period and damping.

Rolling moment due to yawing.- The variation of rolling-moment coefficient due to yawing velocity,  $C_{l_r}$ , with lift coefficient was determined from figure 26 and equation (37) of reference 8 for the wing alone. Corrections for compressibility effects were applied by means of equation (15) of reference 6.

The increment of  $C_{l_r}$  due to the vertical tail was found by means of the following expression:

$$(C_{l_r})_v = - \frac{2l_{v_r}}{b^2} (z_{v_r} - l_{v_r} \sin \alpha) (C_{Y_\beta})_v \quad (A6)$$

For the airplane,  $C_{l_r}$  is given as:

$$C_{l_r} = (C_{l_r})_w + (C_{l_r})_v \quad (A7)$$

Yawing moment due to yawing.- The yawing-moment coefficient due to yawing velocity,  $C_{n_r}$ , was determined for the wing alone as a function of lift coefficient from figures 14 and 27 and equation (41) of reference 8.

The contribution of the vertical tail was computed as a function of Mach number from the following relation:

$$(C_{n_r})_v = 2 \left( \frac{l_{vr}}{b} \right)^2 (C_{Y\beta})_v \quad (A8)$$

For each lift coefficient and Mach number considered, the estimated value of  $C_{n_r}$  for the airplane is given as:

$$C_{n_r} = (C_{n_r})_w + (C_{n_r})_v \quad (A9)$$

The center of pressure of the vertical tail used to determine  $z_{v_r}$  was obtained from figure 5 of reference 9, using the aspect ratio, taper ratio, and sweep angle of the vertical tail, the root of which was assumed to lie on the fuselage reference axis. The center of pressure was assumed to lie on the quarter-chord line.

The lateral-force coefficients due to rolling and yawing velocities,  $C_{y_p}$  and  $C_{y_r}$ , were found to have little effect on the computed lateral motion of the test airplane. Therefore, those derivatives were assumed to be equal to zero in this analysis.

## REFERENCES

1. Thompson, Jim Rogers, Bray, Richard S., and Cooper, George E.: Flight Calibration of Four Airspeed Systems on a Swept-Wing Airplane at Mach Numbers Up to 1.04 by the NACA Radar-Phototheodolite Method. NACA RM A50H24, 1950.
2. Sternfield, Leonard: Effect of Product of Inertia on Lateral Stability. NACA TN 1193, 1947.
3. Letko, William, and Riley, Donald R.: Effect of an Unswept Wing on the Contribution of Unswept-Tail Configurations to the Low-Speed Static- and Rolling-Stability Derivatives of a Midwing Airplane Model. NACA TN 2175, 1950.
4. Anon.: Flying Qualities of Piloted Airplanes. U.S. Air Force Spec. No. 1815-B, June 1, 1948.
5. Kauffman, William M., Liddell, Charles J., Jr., Smith, Allan, and Van Dyke, Rudolph D., Jr.: An Apparatus for Varying Effective Dihedral in Flight with Application to a Study of Tolerable Dihedral on a Conventional Fighter Airplane. NACA Rep. 948, 1949. (Formerly NACA TN's 1936 and 1788.)
6. Fisher, Lewis R.: Approximate Corrections for the Effects of Compressibility on the Subsonic Stability Derivatives of Swept Wings. NACA TN 1854, 1949.
7. DeYoung, John: Theoretical Antisymmetric Span Loading for Wings of Arbitrary Plan Form at Subsonic Speeds. NACA TN 2140, 1950.
8. Toll, Thomas A., and Queijo, M. J.: Approximate Relations and Charts for Low-Speed Stability Derivatives of Swept Wings. NACA TN 1581, 1948.
9. DeYoung, John, and Harper, Charles W.: Theoretical Symmetric Span Loading at Subsonic Speeds for Wings Having Arbitrary Plan Form. NACA Rep. 921, 1948. (Formerly NACA TN's 1476, 1491, 1772.)

TABLE I.- DIMENSIONS OF TEST AIRPLANE

Wing	
Area . . . . .	287.9 sq ft
Span . . . . .	37.12 ft
Aspect ratio . . . . .	4.785
Taper ratio . . . . .	0.513
Dihedral . . . . .	3°
Sweepback of 0.25-chord line . . . . .	35°14'
Root airfoil section (normal to 0.25-chord line) . . .	NACA 0012-64 (modified)
Tip airfoil section (normal to 0.25-chord line) . . .	NACA 0011-64 (modified)
Horizontal Tail	
Area . . . . .	35.0 sq ft
Span . . . . .	12.75 ft
Aspect ratio . . . . .	4.65
Taper ratio . . . . .	0.450
Sweepback of 0.25-chord line . . . . .	34°35'
Airfoil section (parallel to center line) . . . . .	NACA 0010-64
Vertical Tail	
Area . . . . .	39.75 sq ft
Span . . . . .	8.38 ft
Aspect ratio . . . . .	1.77
Taper ratio . . . . .	0.345
Sweepback of 0.25-chord line . . . . .	35°

TABLE II.- PARAMETERS USED IN COMPUTING LATERAL PERIOD, DAMPING, AND

$$\frac{|\phi|}{|\beta|}$$

$h_p$	M	$C_L$	$C_{L\alpha}$	$\alpha_0$	$C_{L\beta}$	$C_{n\beta}$	$C_{Y\beta}$	$^a C_{Lp}$	$^b C_{Lp}$	$^a C_{np}$	$^b C_{np}$	$C_{Lr}$	$C_{nr}$	$a_P$	$b_P$	$^a T_{1/2}$	$^b T_{1/2}$	$^a \frac{ \phi }{ \beta }$	$^b \frac{ \phi }{ \beta }$
10,000	0.35	0.351	0.0693	-0.25	-0.0836	0.1060	-0.680	-0.3486	-0.3490	-0.0235	-0.0308	0.122	-0.1770	2.44	2.43	2.23	2.30	1.59	1.58
	.45	.211	.0710	-.40	-.0684	.1088	-.686	-.3540	-----	-.0140	-----	.097	-.1795	1.92	-----	1.77	-----	1.28	-----
	.55	.142	.0733	-.40	-.0590	.1123	-.696	-.3620	-----	-.0093	-----	.086	-.1840	1.57	-----	1.42	-----	1.06	-----
	.65	.101	.0768	-.40	-.0565	.1170	-.708	-.3700	-----	-.0065	-----	.080	-.1887	1.30	-----	1.17	-----	0.96	-----
	.75	.076	.0824	-.40	-.0565	.1233	-.724	-.3800	-.3860	-.0049	-.0026	.077	-.1953	1.11	1.11	0.98	0.98	0.90	0.90
35,000	.55	.412	.0733	-.40	-.0927	.1123	-.696	-.3620	-.3640	-.0270	-.0358	.142	-.1835	2.56	2.55	3.85	4.08	2.01	1.99
	.70	.255	.0791	-.40	-.0773	.1199	-.715	-.3750	-----	-.0160	-----	.116	-.1896	2.02	-----	3.06	-----	1.61	-----
	.80	.195	.0869	-.40	-.0741	.1273	-.733	-.3850	-----	-.0120	-----	.108	-.1970	1.73	-----	2.63	-----	1.45	-----
	.90	.154	.0943	-.25	-.0721	.1366	-.757	-.3990	-----	-.0092	-----	.106	-.2065	1.49	-----	2.21	-----	1.31	-----
	1.00	.125	.0785	-.50	-.0768	.1467	-.782	-.4140	-.4190	-.0068	-.0047	.104	-.2170	1.30	1.30	1.89	1.87	1.30	1.23

aValues computed for wing alone.

bValues for wing plus vertical tail contribution computed by method of reference 3.

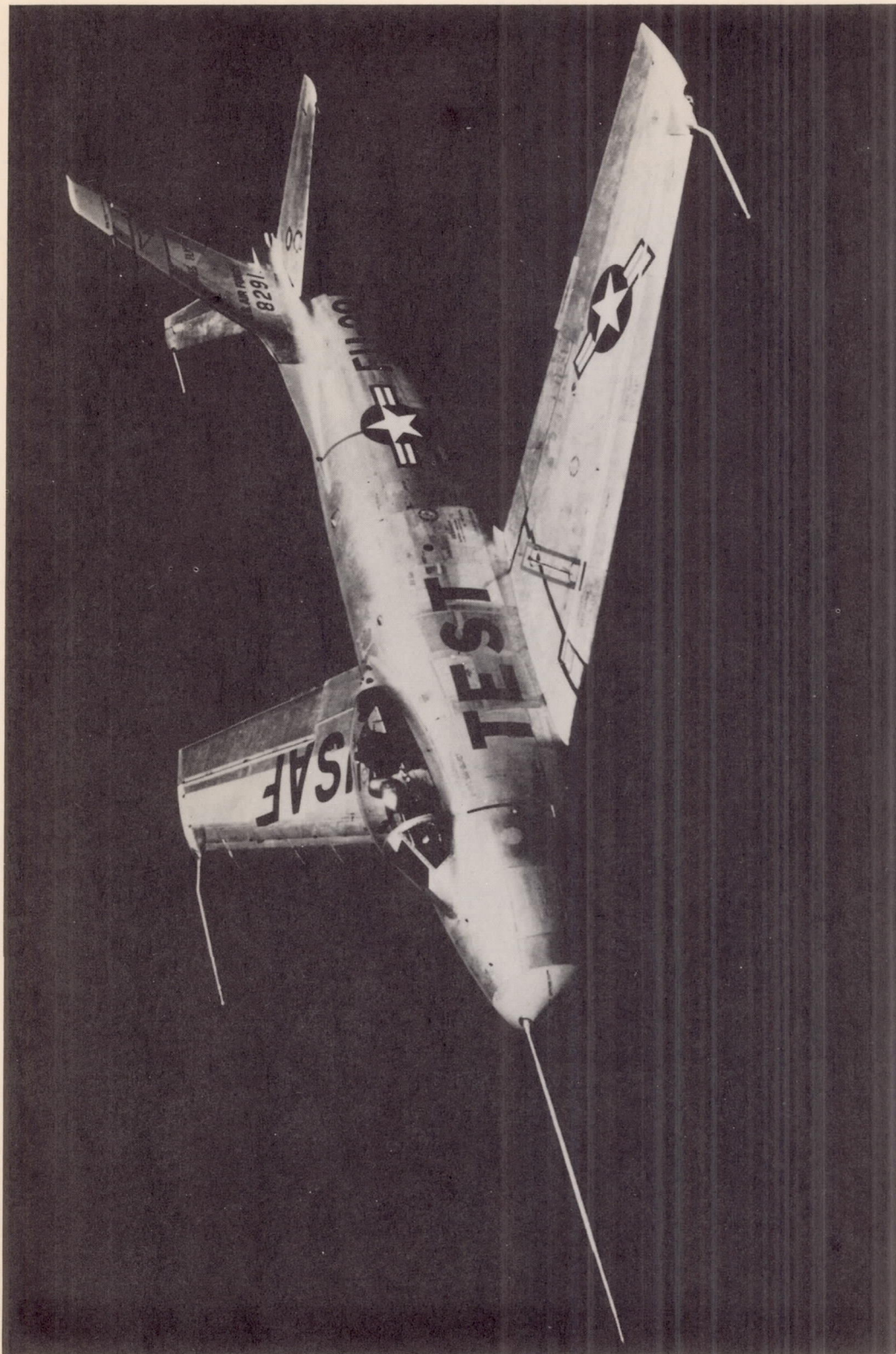
Constants:  $W = 12,500$      $I_x = 7245$      $C_{Yp} = 0$   
 $S = 287.9$      $I_z = 23,191$      $C_{Yr} = 0$   
 $b = 37.12$      $\epsilon = 2.5$

TABLE III.- AVERAGE VALUES OF THE MEASURED LATERAL OSCILLATORY CHARACTERISTICS OF TEST AIRPLANE AT VARIOUS MACH NUMBERS FOR ALTITUDES OF 10,000 AND 35,000 FEET

$h_p$	M	P	$T_{1/2}$	$\frac{ \phi }{ \beta }$
10,000	0.40	2.14	2.05	1.95
	.50	1.70	1.60	1.70
	.60	1.38	1.35	1.49
	.70	1.15	1.27	1.30
	.79	1.00	1.21	1.15
35,000	.50	2.55	4.10	2.48
	.60	2.23	3.50	2.07
	.70	1.95	2.92	1.91
	.80	1.70	2.44	1.77
	.90	1.50	1.85	1.64
	1.00	1.34	1.76	1.52
	1.04	1.27	2.00	1.48







A-15020

Figure 1.- Photograph of the test airplane.

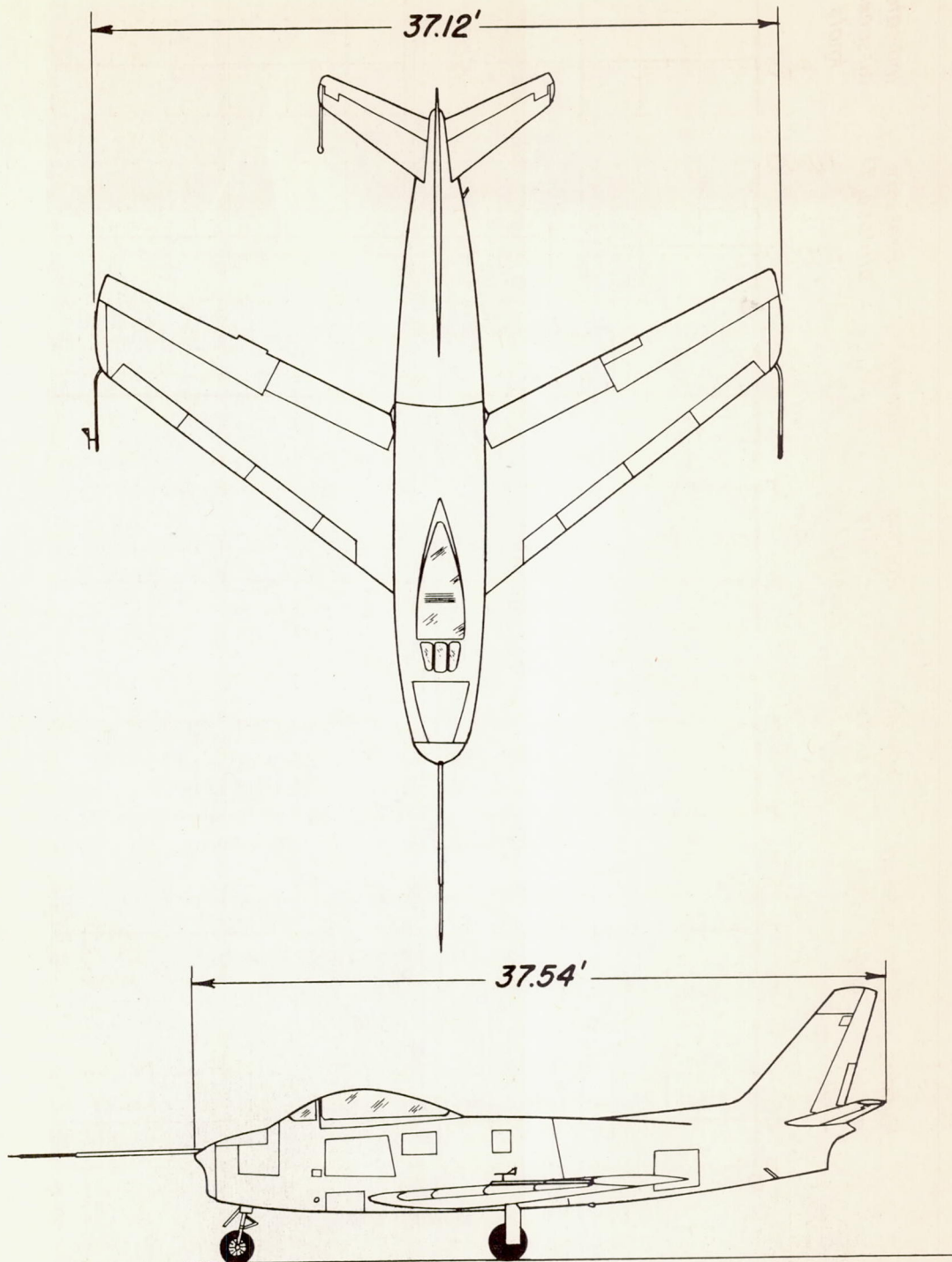


Figure 2.- Two-view drawing of the test airplane.

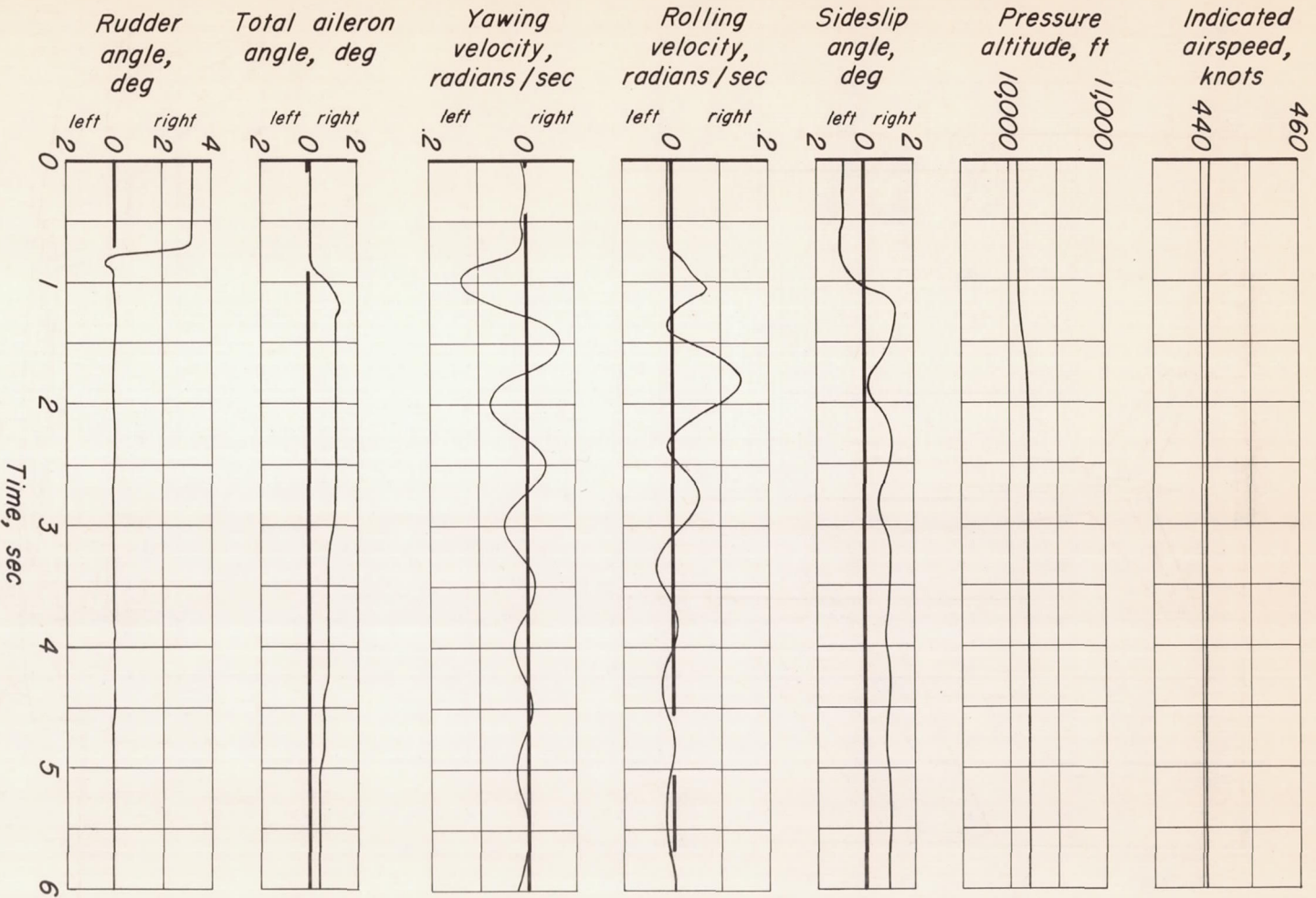


Figure 3.- Time histories of measured quantities during lateral oscillation; Mach number, 0.79; pressure altitude, 10,000 feet.

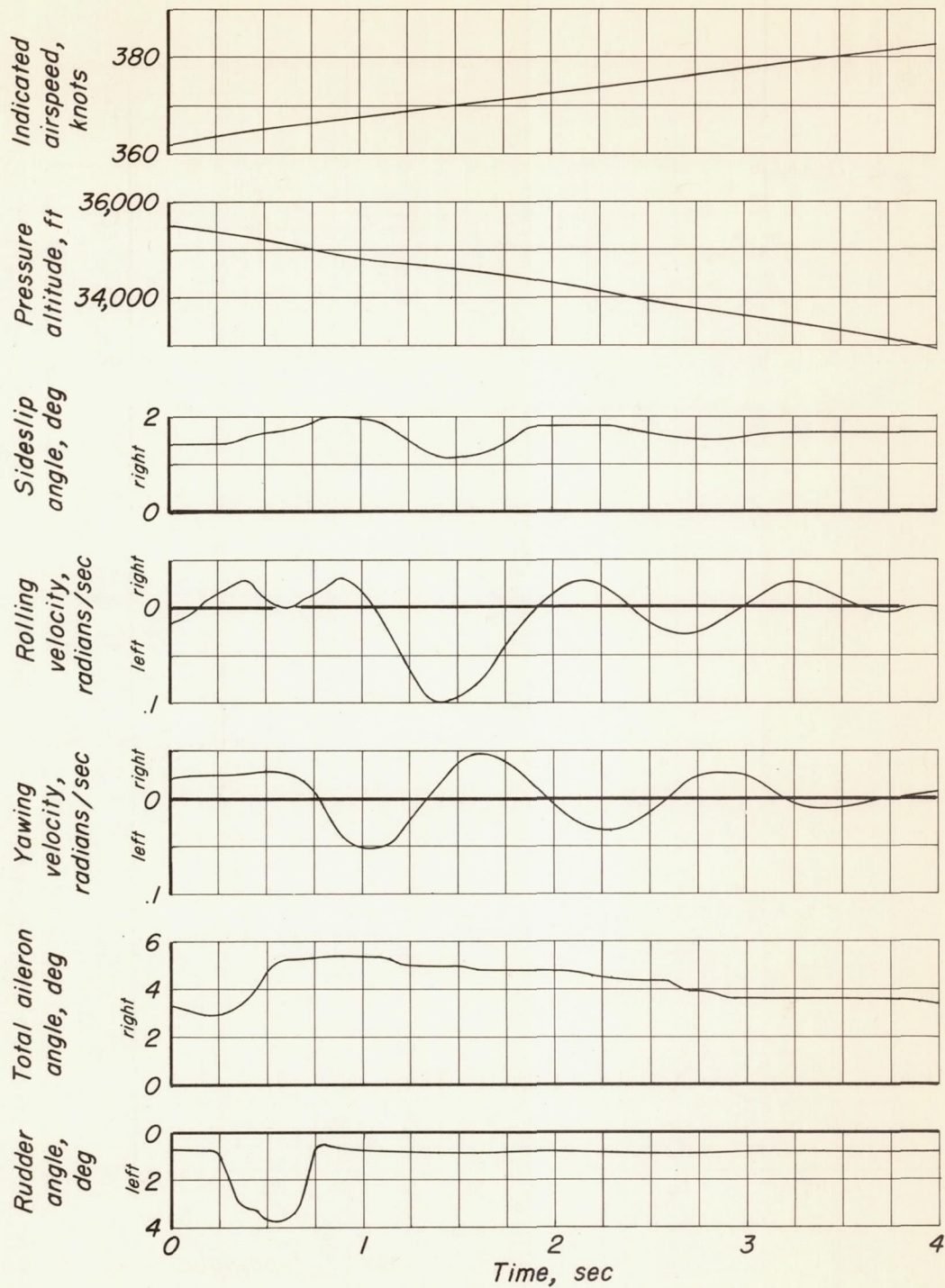


Figure 4.- Time histories of measured quantities during lateral oscillation; Mach number, 1.04; pressure altitude, 35,000 feet.

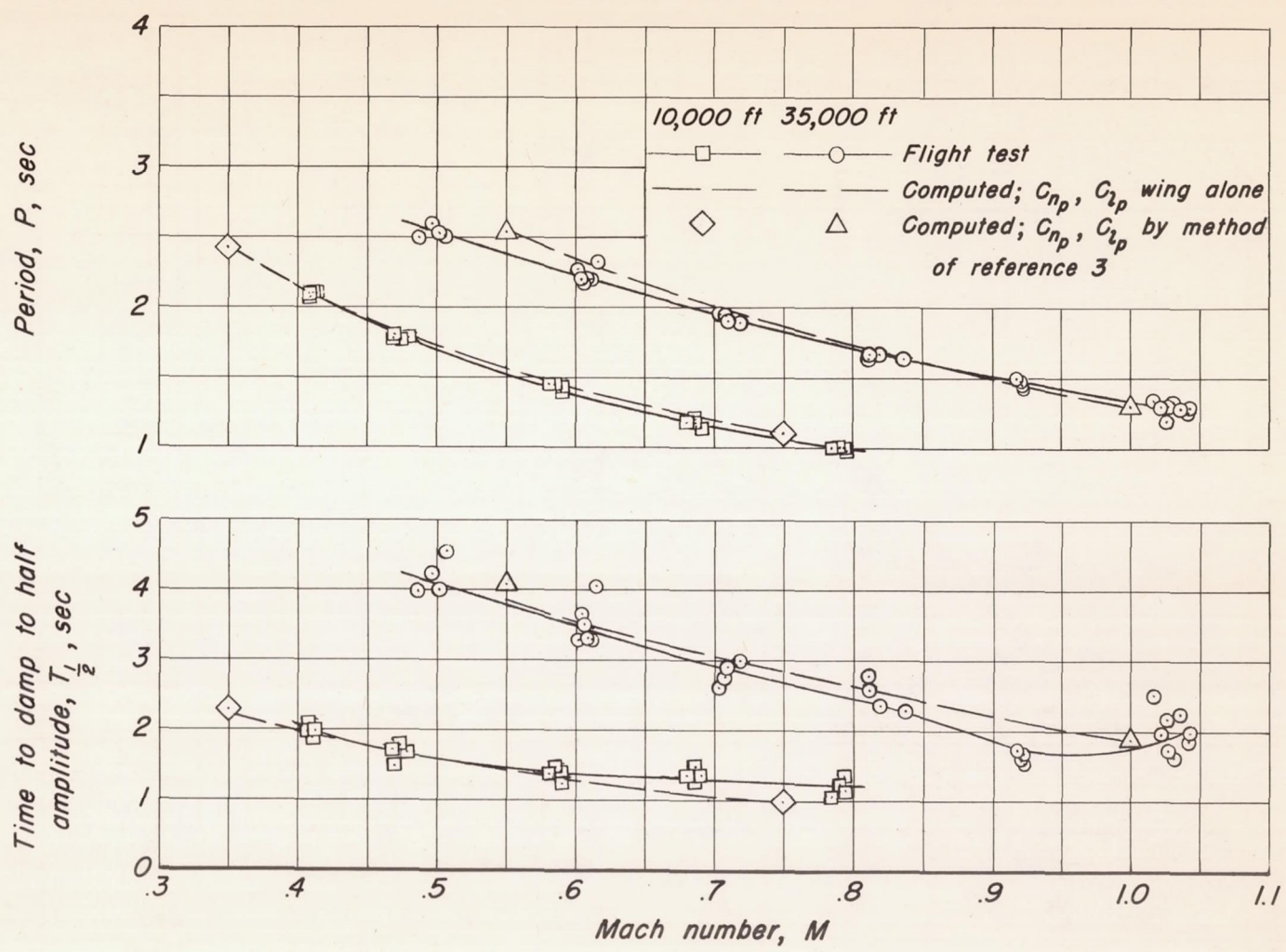


Figure 5.- Variation with Mach number of experimental and computed lateral period and damping characteristics at each test altitude.

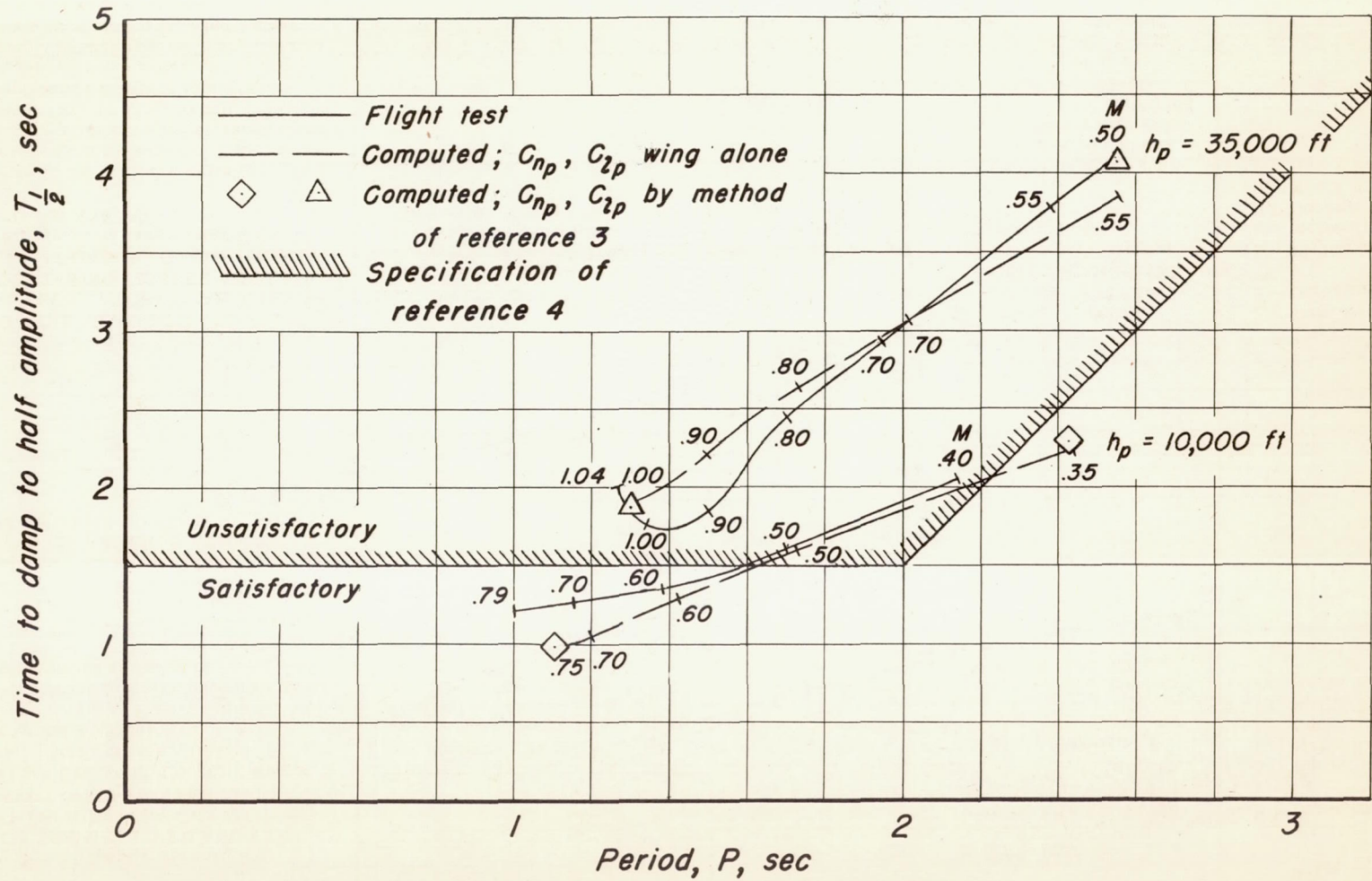


Figure 6.- Comparison of experimental and computed lateral period-damping relationships with Armed Services specification dated 1948.